Aalborg Universitet

An Improved Anisotropic Vector Preisach Hysteresis Model Taking Account of Rotating Magnetic Fields

Zhu, Lixun; wu, weimin; Xu, XIaoyan; Guo, Yi; Li, Wei; Lu, Kaiyuan; Koh, Chang-Seop

An Improved Anisotropic Vector Preisach Hysteresis Model Taking Account of Rotating Magnetic Fields

Lixun Zhu[1], Weimin Wu[1], Xiaoyan Xu[1], Yi Guo[1], Wei Li[2], Kaiyuan Lu[1,3], and Chang-Seop Koh[4]

[1]Department of Logistics Engineering, Shanghai Maritime University, Shanghai 201306, China
[2]Department of Electrical Engineering, Tongji University, Shanghai 200092, China
[3]Department of Energy Technology, Aalborg University, 9220 Aalborg, Denmark
[4]Department of Electrical and Computer Engineering, Chungbuk National University, Cheongju 28644, South Korea

This paper presents an identification algorithm of the scalar Preisach model by using a set of symmetric minor hysteresis loops and suggests an improved vector Preisach model to describe the vector and anisotropic hysteresis behavior of a non-oriented (NO) electrical steel sheet (ESS) under rotating magnetic fields. Symmetric minor hysteresis loop is quite easy measured, so an identification algorithm based on symmetric minor hysteresis loop instead of first-order reverse curve is presented in this paper. The vector Preisach model employs a nonlinear coefficient, which is a function of magnitude and a direction of magnetic flux density, to describe the anisotropic property of the NO ESS and increases the numerical accuracy. The validity of the suggested vector Preisach model is investigated through comparisons with the experimental results under various magnetic field conditions.

Index Terms—**Electrical steel sheet (ESS), hysteresis model, vector hysteresis property, vector preisach model.**

I. INTRODUCTION

MOST electrical machines have both rotating magnetic fields and alternating fields, and combination of them results vector hysteresis behaviors. Therefore, magnetic field finite-element analyses and iron loss calculation of the electrical machines require accurate description of the vector hysteresis property of the electrical steel sheet (ESS). Up until now, several vector hysteresis models [1]–[4] have been proposed to describe the vector hysteresis properties under alternating and rotating magnetic fields. However, even if so many vector hysteresis models have been developed, the accuracy and the efficiency of the developed models are not satisfied.

The scalar Preisach model is considered numerically efficient and accurate. As we all known, the Everett function should accurately be identified by using first-order reverse curve (FORC) traditionally. However, the process of FORC measurement is quite difficult and tedious, and the measured data must be modified to get the reasonable results [5]. The vector Preisach model is superposition of the scalar Preisach models along the azimuthal direction [1]. However, the traditional vector Preisach model cannot consider the anisotropic property of the ESS. Therefore, Dlala *et al.* [5] and Kuczmann [6] tried to describe the anisotropic property. However, the comparisons of their outputs with experimentally measured data show that the accuracy of the anisotropic versions is still not satisfactory to be applied to electric machines such as motors and generators [6].

In this paper, an identification algorithm of the scalar Preisach model is proposed to improve the accuracy. A set of symmetric minor loops that have different maximum values

of magnetic flux density ($B_{\max}$) will be adopted to identify the Everett function of the scalar Preisach model. Then, an improved anisotropic vector Preisach model is developed to describe the anisotropic vector magnetic properties of the non-oriented (NO) ESS under rotating magnetic fields. The proposed anisotropic vector Preisach model increases modeling accuracy, especially under rotating magnetic fields. Although applications to NO ESS, 35PN440, and comparison of the results with experimentally measured ones, the effectiveness of the proposed model is investigated.

II. SCALAR PREISACH MODEL AND ITS IDENTIFICATION

A. Scalar Preisach Model

An inverted version of the scalar Preisach model, which provides its output magnetic field strength (H) from the input magnetic flux density (B), is expressed as follows:

$$H = \Gamma(B) = \iint_{\alpha \geq \beta} \mu(\alpha, \beta) \gamma_{\alpha\beta}(B(t)) d\alpha d\beta \quad (1)$$

where $\gamma_{\alpha\beta}$ is a hysteresis operator controlled by the increasing α and decreasing β values of the input B and μ is the distribution function of the hysteresis operators. The hysteresis operator is given as

$$\gamma_{\alpha\beta}(B(t_k)) = \begin{cases} +1 & \text{if } B(t_k) > \alpha \\ -1 & \text{if } B(t_k) < \beta \\ \gamma_{\alpha\beta}(B(t_{k-1})) & \text{if } \beta \leq B(t_k) \leq \alpha \end{cases} \quad (2)$$

where t_k is the instance time step of input B.

From the definition of the scalar Preisach model, the integral area of (1) is a triangle as shown in Fig. 1, and it is called the Preisach plane. According to the input B-waveform, the Preisach plane can be separated to the positive $T^+(t)$ and negative $T^-(t)$ parts whose output values of the hysteresis operators are $+1$ and -1, respectively. The shape of the stair line is a function of the input B-waveform, and it depends on the history of the input B-waveform.
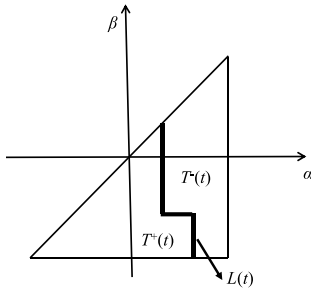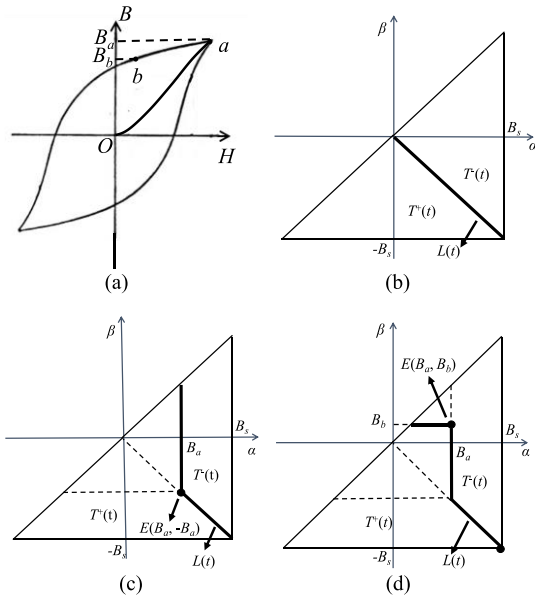
Fig. 1. Preisach plane.

(a) (b)

(c) (d)

Fig. 2. Symmetric minor loop when $B_{\max} = a$ and the corresponding Preisach plane. (a) Symmetric minor loop. (b) Preisach plane at the initial point O. (c) Preisach plane when $B = B_a$. (d) Preisach plane when $B = B_b$.

To improve the calculation efficiency of (1), the Everett function at point (α_0, β_0) is defined to instead the double-integral calculation in (1) as follows:

$$E(\alpha_0, \beta_0) = \iint_{\alpha < \alpha_0, \beta > \beta_0} \mu(\alpha, \beta) d\alpha d\beta. \tag{3}$$

Therefore, (1) can be instead by addition and subtraction of the Everett function.

B. Identification Method

From (1) and (3), the Everett function should be identified instead of the distribution function. Fig. 2(a) shows a symmetric minor loop whose $B_{\max} = B_a$ at point a. In Fig. 2(a), point O is the initial point, and the corresponding Preisach plane is shown in Fig. 2(b). Then, if B increases to point a whose $B_{\max} = B_a$, the corresponding Preisach plane is shown in Fig. 2(c). According to (3), the Everett function at point $(E_a, -E_a)$ can be calculated as

$$E(B_a, -B_a) = B_a. \tag{4}$$

Next, B is decreased from point a to point b, then, the corresponding Preisach plane as shown in Fig. 2(d), and the Everett function at point (E_a, E_b) can be calculated as
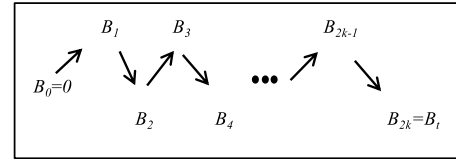
$$E(B_a, B_b) = (B_a - B_b)/2. \tag{5}$$

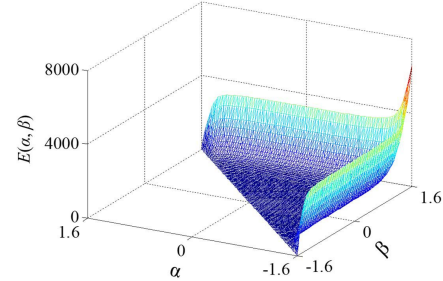Fig. 3. Hysteresis operator of the Preisach model.

Fig. 4. Everett function of 35PN440.

Similarly, the Everett function on the line $\alpha = B_a$ from point (E_a, E_a) to point $(E_a, -E_a)$ can be calculated by using the upper branch of the minor loop.

The proposed identification method can be summarized as follows.

Step 1: Calculate the Everett function along the line $\alpha = -\beta$. by using the $B_{\max}$ point of each minor loop and (4).

Step 2: Calculate the Everett function in the upper triangle zone of the Preisach plane by using the upper branch of each minor loop and (5).

Because the Everett function is symmetric with $\alpha = -\beta$, the lower triangle zone of the Preisach plane can be obtained from the upper triangle.

C. Implementation and Application Results

The result of the scalar Preisach model is decided by the shape of the stair line. Therefore, the shape of the stair line should be recorded. In this paper, an extreme point memory as shown in Fig. 3 is adopted to record each extreme point of the B-waveform, and (1) can be rewritten as

$$H(t) = \begin{cases} \text{sign}(B_2 - B_1) \cdot E(|B_2|, -|B_2|) + \\ 2\sum_{k=3}^{N} \begin{cases} E(B_k, B_{k-1}) \\ \quad \text{when sign } (B_k - B_{k-1}) > 0 \quad k > 1 \\ -E(B_{k-1}, B_k) \\ \quad \text{when sign } (B_k - B_{k-1} =) < 0 \end{cases} \\ 0 \qquad\qquad\qquad\qquad\qquad\qquad\qquad\qquad k = 1 \end{cases} \tag{6}$$

where B_k is the extreme point in the extreme point memory.

The proposed identification algorithm is applied to an NO ESS 35PN440 specimen. Totally, 16 symmetric B–H loops are measured along the rolling direction for the range of $0.1 \leq B \leq 1.6$ (T) by using 2-D single-sheet tester [7], and then, the Everett function is identified.

Fig. 4 shows the Everett function which identified by the proposed method. Fig. 5 shows the application results to minor loops under alternating magnetic fields along the rolling direction where modeling results match well with the measured ones.
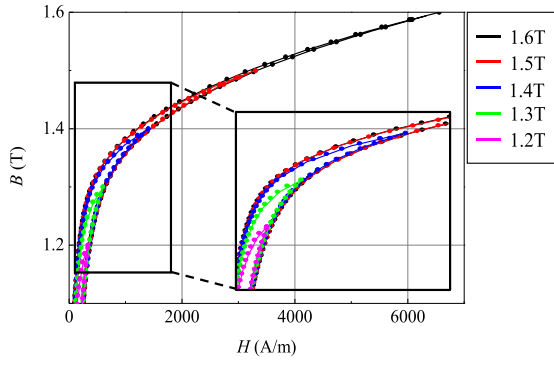
Fig. 5. Comparison of the measured (dotted line) and modeled (solid line) major loop ($B_{max} = 1.6$ T) and minor loos under alternating magnetic field along the rolling direction.

III. ANISOTROPIC VECTOR PREISACH MODEL

A. Original Anisotropic Vector Preisach Model

The original vector Preisach model that can consider the anisotropic property of ESS has been proposed as follows:

$$\mathbf{H} = \int_{-\pi/2}^{\pi/2} \mathbf{e}_{\varphi_i} H_{\varphi_i}(B_{\varphi_i}) d\varphi \qquad (7\text{-}a)$$

$$H_{\varphi_i}(B_{\varphi_i}) = \iint_{\alpha \geq \beta} \eta(\alpha', \beta') \hat{\gamma}(B_{\varphi_i}) d\alpha' d\beta' \qquad (7\text{-}b)$$

$$B_{\varphi_i} = |\mathbf{B}|\delta|\cos(\theta_B - \varphi_i + \psi)|^{1/\omega} \qquad (7\text{-}c)$$

where $H_{\varphi i}$ is calculated from the scalar Preisach model along the φ_i direction, having the flux density $B_{\varphi i}$ as input, η is the vector distribution function, and $\delta = \text{sign}[\cos(\theta_B - \varphi_i + \psi)]$, ω is a parameter to generate the flower shape of **H**-waveform to describe the anisotropic property, and ψ is a parameter to control the initial phase of the **H**-waveform. They are decided by fitting the measured data.

It should be noted that the original model cannot match the measured **H**-waveforms very well under rotating magnetic fields, although it can generate flower shaper **H**-waveforms by using parameter ω.

B. Improved Anisotropic Vector Preisach Model

This paper proposes a new simple anisotropic vector Preisach model as follows:

$$\mathbf{H} = \int_{-\pi/2}^{\pi/2} \mathbf{e}_{\varphi_i} H_{\varphi_i}(B_{\varphi_i}) d\varphi \qquad (8\text{-}a)$$

$$H_{\varphi_i}(B_{\varphi_i}) = z(|\mathbf{B}|, \varphi_i) \iint_{\alpha \geq \beta} \eta(\alpha', \beta') \hat{\gamma}(B_{\varphi_i}) d\alpha' d\beta' \qquad (8\text{-}b)$$

$$B_{\varphi_i} = |\mathbf{B}| \cos(\theta_B - \varphi_i + \psi(B_{max})) \qquad (8\text{-}c)$$

where z is a parameter to describe the anisotropic property, and it is a function of $|\mathbf{B}|$ and φ_i, and $\psi(B_{max})$ is also used to control the initial phase of the H-waveforms. This is motivated by the experimental phenomena that the shape and the initial phase of the H-waveforms are quite different under the circle magnetic fields with a different B_{max}.

Similar with the scalar Everett function $E(\alpha, \beta)$, the vector Everett function $F(\alpha', \beta')$ is used to implemented the vector
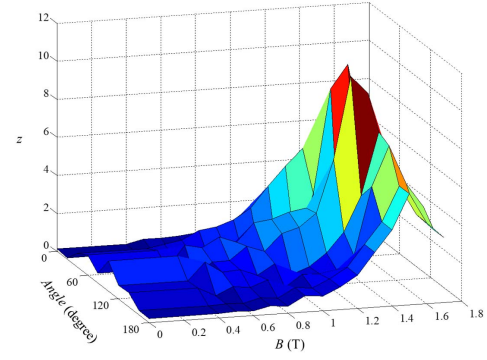
(a)
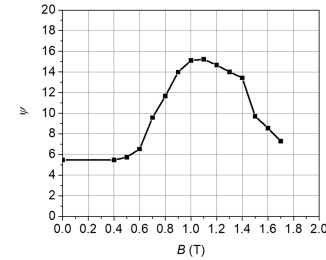
(b)

Fig. 6. Parameters z and ψ for 35PN440.

Preisach model, and it can be identified from the scalar Everett function as follows:

$$F(\alpha, \beta) = \int_{-\pi/2}^{\pi/2} \cos\varphi \, E(\alpha\cos\varphi, \beta\cos\varphi) d\varphi. \qquad (9)$$

To implement the improved anisotropic vector Preisach model, (8-a) should be rewritten to its discrete format as

$$\mathbf{H} = \sum_{i=1}^{n} H_{\varphi_i}(B_{\varphi_i}) \omega_i \qquad (10)$$

where ω_i is the weight of Gauss integral method, and (9) can be solved by using the method which is explained in [7].

The parameters z and ψ are identified via fitting the measured **H**-waveforms under different B_{max} circle magnet fields and by using the particle swarm optimization method.

C. Modeling Results

The proposed vector anisotropic model was applied to predict **H**-waveforms when alternating and rotating magnetic flux densities are applied to NO ESS (35PN440). The coefficients z and ψ in (8) are constructed by using a set of measured **H**-waveforms under circular rotating magnetic flux density for the range of $0.4 \leq B \leq 1.6$ (T) as shown in Fig. 6.

Fig. 7 shows the comparisons of the measured and predicted H-waveforms using the original and proposed vector hysteresis model under circular rotating magnetic field conditions when $B_{max} = 1.6$ T. From Fig. 7, the accuracy of the proposed method is much better than the original one.

To compare the modeling accuracy, deviation between the measured and modeling results under different B_{max} rotating magnetic fields, $d_{H,k}(\%)$, is defined as follows:

$$d_{H,k} = \frac{\sqrt{\sum_{i=1}^{N}\left(H_k^{mea}(\tau_i) - H_k^{mod}(\tau_i)\right)^2}}{N\{\max(H^{mea}) - \min(H^{mea})\}} \times 100 \ [\%] \qquad (11)$$
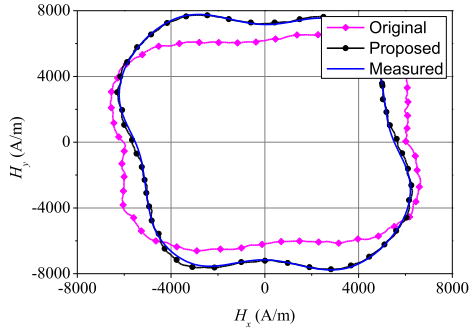
Fig. 7. Modeling results comparison of original method, proposed method, and measured data under circle magnetic field when $B_{max} = 1.6$ T.

TABLE I

COMPARISON OF MODELING ACCURACIES WHEN $B_{max} = 1.6$ T

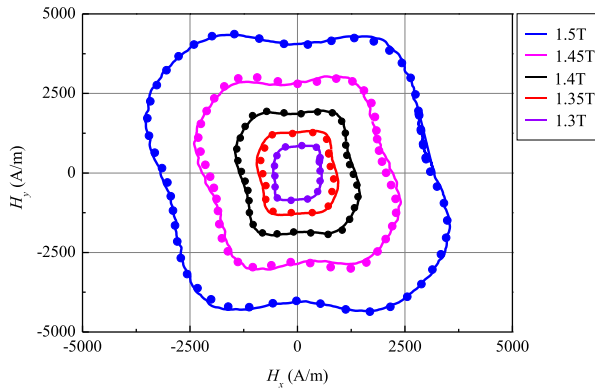| $d_{H,k}$ (%)	H_x-waveform	H_y-waveform
Original model	59.33	69.17
Improved model	9.21	7.39

Fig. 8. Modeling results comparison of original method, proposed method, and measured data under different B_{max} circle magnetic fields.

where k refers x, y, N is the number of sampling points of a H-waveform, τ stands for $\omega t \in [0, 2\pi]$ with as the angular frequency of a B-waveform, and H_{mea} and H_{mod} are the measured and modeling H-waveforms, respectively. Table I shows the modeling accuracies of original and improved model when $B_{max} = 1.6$ T under rotating magnetic field. From Table I, the improved model gives a better accuracy than the original one.

Fig. 8 shows the comparisons of the measured and predicted H-waveforms using the proposed model under circular rotating magnetic field conditions. In Fig. 8, the H-waveforms for $B_{max} = 1.3$, 1.4, and 1.5 T are used in the calculation of z and ψ, while those for $B_{max} = 1.35$ and 1.45 T are not. It means the proposed vector hysteresis model can describes the behaviors of the H-waveforms very accurately under various rotating magnetic fields.

The H-waveform predicted by the proposed vector hysteresis model for an alternating magnetic field of $B_{max} = 1.5$ T is shown in Fig. 9 together with those from measured and the original vector Preisach model. It means the proposed vector hysteresis model automatically reduces to scalar model.
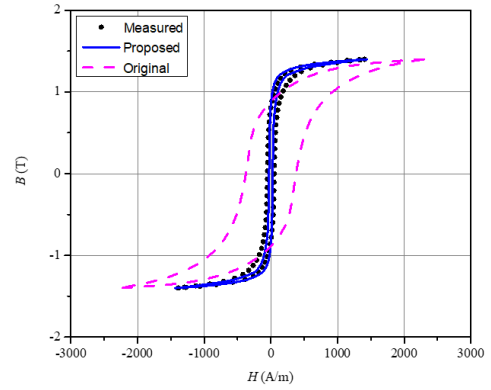

Fig. 9. Modeling results comparison of the proposed method and measured data under alternating magnetic fields along the rolling direction when $B_{max} = 1.4$ T

IV. CONCLUSION

An improved anisotropic vector Preisach hysteresis model is proposed to describe the anisotropic behavior of NO ESS under rotating magnetic fields. The proposed model is improved from the conventional model by introducing two coefficients, z and ψ, which can be identified by using measured H-waveforms under circular magnetic fields conditions. An improved identification method for scalar play model is also proposed, and a set of different B_{max} symmetric minor loops is used to identify the scalar Everett function. Through applications to NO ESS, the proposed vector hysteresis model is proven to describe the anisotropic properties under various rotating magnetic fields.

REFERENCES

[1] E. Fallah and J. S. Moghani, "A new identification and implementation procedure for the isotropic vector Preisach model," *IEEE Trans. Magn.*, vol. 44, no. 1, pp. 37–42, Jan. 2008.

[2] W. Li, I. H. Kim, S. M. Jang, and C. S. Koh, "Hysteresis modeling for electrical steel sheets using improved vector Jiles-Atherton hysteresis model," *IEEE Trans. Magn.*, vol. 47, no. 10, pp. 3821–3824, Oct. 2011.

[3] L. Zhu and C. S. Koh, "A novel vector hysteresis model using anisotropic vector play model taking into account rotating magnetic fields," *IEEE Trans. Magn.*, vol. 53, no. 6, Jun. 2017, Art. no. 7300604.

[4] H. Yoon, I. Kim, P. S. Shin, and C. S. Koh, "Finite element implementation of a generalized Chua-type vector hysteresis model and application to iron loss analysis of three-phase transformer," *IEEE Trans. Magn.*, vol. 47, no. 5, pp. 1122–1125, May 2011.

[5] E. Dlala, A. Belahcen, K. A. Fonteyn, and M. Belkasim, "Improving loss properties of the Mayergoyz vector hysteresis model," *IEEE Trans. Magn.*, vol. 46, no. 3, pp. 918–924, Mar. 2009.

[6] M. Kuczmann, "Measurement and simulation of vector hysteresis characteristics," *IEEE Trans. Magn.*, vol. 45, no. 11, pp. 5188–5191, Nov. 2009.

[7] L. Zhu, H.-S. Yoon, H.-J. Cho, D.-J. Um, and C.-S. Koh, "Finite-element analysis of magnetostriction force in power transformer based on the measurement of anisotropic magnetostriction of highly grain-oriented electrical steel sheet," *IEEE Trans. Magn.*, vol. 52, no. 3, Mar. 2016, Art. no. 6100304.